

Electronic Supplementary Information

Sequential growth of iridium cluster anions based on simple cubic packing

Kiichirou Koyasu,^{1,2*} Ryohei Tomihara,¹ Toshiaki Nagata,³ Jenna W. J. Wu,³ Motoyoshi Nakano,³ Keijiro Ohshima,³ Fuminori Misaizu,^{3*} and Tatsuya Tsukuda^{1,2*}

¹ Department of Chemistry, School of Science, The University of Tokyo, 7-3-1 Hongo, Bunkyo-ku, Tokyo 113-0033, Japan

² Elements Strategy Initiative for Catalysts and Batteries (ESICB), Kyoto University, 1-30 Goryo-Ohara, Nishikyo-ku, Kyoto 615-8245, Japan

³ Department of Chemistry, Graduate School of Science, Tohoku University, 6-3 Aoba, Aramaki, Aoba-ku, Sendai 980-8578, Japan

E-mails: kkoyasu@chem.s.u-tokyo.ac.jp, misaizu@tohoku.ac.jp, tsukuda@chem.s.u-tokyo.ac.jp

Methods

IMMS measurement was conducted by using the apparatus installed at Tohoku University,^{1,2} which consists of three parts: a cluster source, an ion drift cell, and a time-of-flight mass spectrometer (TOF-MS) equipped with a reflectron. Iridium cluster anions Ir_n^- were generated by a laser vaporization (LV) method with the output of the second harmonic of a Nd:YAG laser (532 nm) onto a rotating and translating Ir rod (99.9%, $\phi = 5$ mm) under pulsed He gas (3–6 atm). To measure the collision cross sections, Ir_n^- cluster anions were injected into the ion drift cell filled with He buffer gas (2.00 Torr, ~ 170 K) by a pulsed electric field at a given time ($t = t_0$). An electric field of $E = 10$ V cm⁻¹ was applied to the ion drift cell with a length of 100 mm. The experimental condition was within the low-field condition, in which the ratio of E to the number density of the buffer gas N was $E/N \sim 9$ Td. After exiting the ion drift cell, the ions were reaccelerated at a given time after the first pulse, $t = t_0 + \Delta t$, where Δt is the “arrival time,” and a series of mass spectra was obtained using the TOF-MS with the reflectron. For the IMMS measurement, a series of TOF mass spectra was obtained sequentially by scanning Δt . Total ion intensity of a certain TOF peak to the arrival time was obtained as a plot of the arrival time distribution.

PES measurement was conducted by using the apparatus installed at the University of Tokyo, which consists of three parts: a cluster source followed by a reaction cell, a TOF-MS, and a magnetic-bottle type photoelectron energy analyzer.^{1,3} Ir_n^- was also generated by LV with He carrier gas (6 atm). The stainless-steel tubes for He carrier gas were baked-out to reduce residual water, thereby significantly suppressing the generation of oxide impurities. The generated cluster anions were perpendicularly extracted and analyzed by a linear TOF-MS. The mass-selected product anion was irradiated by the fourth harmonic of a Nd:YAG laser. The energy of the detached photoelectrons was analyzed by MB-PES with a flight path of 1.47 m. The spectra were calibrated using that of Au^- (Ref. 4) and the calibrated spectrum of Ir_6^- on each measurement. Background signals without clusters were subtracted from each count, measuring photoelectron signals at 10 Hz. The spectra presented in this paper were obtained by accumulating 5000–20,000 laser shots and averaging the data with a 0.2 eV window. The resolution of our MB-PES was < 120 meV at the maximum for electrons with a kinetic energy of 1.0 eV.

The geometric and electronic structures of $\text{Ir}_n^{-/0}$ ($n = 3$ –15) were studied by using the DFT calculations. To reduce the calculation cost, the optimized structures of isomers for collision cross sections were calculated using the TURBOMOLE 7.2 software package⁵ at the

B3LYP/def-SV(P) level with the resolution of the identity approximation. To confirm the relative stabilities of the isomers obtained, BP86 functional has been tested. The BP86 functional has been used for structural optimization of other metal clusters, such as Ru_n clusters.⁶ For the calculation on Ir_7^- , same order for the relative energies were obtained. Adiabatic electron affinity and vertical detachment energy were calculated at the B3LYP/lanl2dz level by using the Gaussian09 software package.⁷ Vibrational frequencies were calculated to confirm that the optimized structures corresponded to the local minimum structures. In the calculation of the relative energies, the zero-point energy was taken into account. VDE was calculated by subtracting the energy of the most stable anion from that of the neutral state with the same structure of the anionic species without considering the zero-point energy.⁸ AEA was obtained from the energy difference between the optimized anion and the optimized neutral species. In the calculations of the VDEs and AEAs, we used the most stable neutral clusters between those with spin multiplicities that differed from that of the anion by ± 1 . The charge on each atom was estimated using natural population analysis. All calculations were carried out using the Gaussian 09 program,⁷ including NBO.⁹ The results were visualized using PyMOL.¹⁰ CCSs of Ir_n^- ($n = 3\text{--}15$) were calculated by applying a projection approximation method to the optimized structures using the MOBCAL software program¹¹, in which CCS was obtained by averaging the results from 20 trials on a randomly rotated target structure with the standard error. For the calculations of CCS, the radii of He and Ir were fixed to 1.15 and 1.89 Å, respectively, by fitting the calculated CCS to the experimentally obtained CCS.

Mass spectrum of iridium cluster anions, Ir_n^-

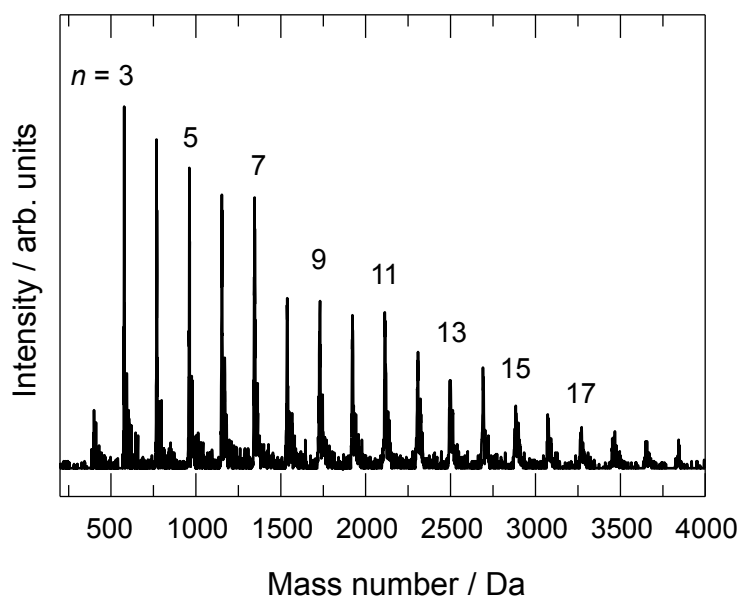


Fig. S1. Typical mass spectrum of Ir_n^- .

Table S1. Relative energies of iridium cluster anions, Ir_n^- ($n = 3\text{--}15$) with different spin multiplicities obtained with TURBOMOLE. Certain spin multiplicities with the lowest relative energy are shown as bolds.

Isomers (odd)	spin multiplicity							
	1	3	5	7	9	11	13	15
3a	0.73	0.30	0.29	0.00	0.51	—	—	—
3b	1.30	0.81	0.57	0.45	0.73	—	—	—
5a	1.26	0.68	0.61	0.57	0.23	0.12	0.00	1.67
5b	5a ^a	5a ^a	1.09	1.12	5a ^a	5a ^a	5a ^a	—
7a	1.34	0.53	0.42	0.29	0.13	0.11	0.06	0.00
7b	1.31	1.06	0.99	0.63	0.48	0.43	0.52	—
7c	1.68	1.33	1.28	0.86	0.86	0.66	0.63	0.68
9a	0.47	0.05	0.00	0.01	0.04	—	—	—
9b	1.35	0.30	0.39	0.32	0.41	—	—	—
9c	1.41	0.66	0.59	0.58	0.61	—	—	—
11a	0.74	0.07	0.13	0.00	0.22	—	—	—
13a	0.84	0.00	0.14	0.15	0.18	—	—	—
13b	0.58	0.06	0.07	0.032	0.028	0.14	—	—
13c	—	—	—	0.252	0.248	0.40	—	—
15a	0.73	0.00	0.05	—	—	—	—	—
15b	0.84	0.15	0.25	—	—	—	—	—
15c	1.36	0.24	0.38	0.34	0.36	—	—	—
7a[†]	—	—	—	—	0.03	0.00	0.04	0.35
7b[†]	—	—	—	—	0.37	0.45	0.64	—
7c[†]	—	—	—	—	0.62	0.61	0.69	0.99

a) transformed into another isomer, [†] Calculated with BP86/ def-SV(P) level.

Isomers (even)	spin multiplicity							
	2	4	6	8	10	12	14	16
4a	0.97	0.78	0.26	0.00	0.02	1.20	—	—
4b	0.66	4a ^a	4a ^a	1.38	—	—	—	—
4c	1.18	1.19	0.89	0.94	1.10	—	—	—
4d	1.71	1.68	4b ^a	4b ^a	—	—	—	—
6a	0.40	0.32	0.19	0.00	0.07	—	—	—
6b	0.43	0.26	0.22	0.123	0.115	0.48	—	—
6c	1.44	1.24	1.09	0.84	0.57	0.2926	0.2928	—
8a	0.06	0.16	0.00	0.10	0.01	—	—	—
8b	1.48	1.75	1.48	1.62	1.42	1.26	1.08	1.11
8c	2.10	2.02	1.89	1.89	1.87	2.11	—	—
10a	0.23	0.05	0.10	0.06	0.00	0.06	—	—
10b	0.25	0.65	0.40	0.19	0.09	0.11	—	—
10c	—	—	—	1.33	1.23	1.50	1.53	—
10d	1.59	1.77	—	—	—	—	—	—
12a	0.005	0.04	0.00	0.12	0.17	—	—	—
14a	0.01	0.05	0.00	0.09	0.14	—	—	—
14b	0.62	0.56	0.61	—	—	—	—	—

a) transformed into another isomer

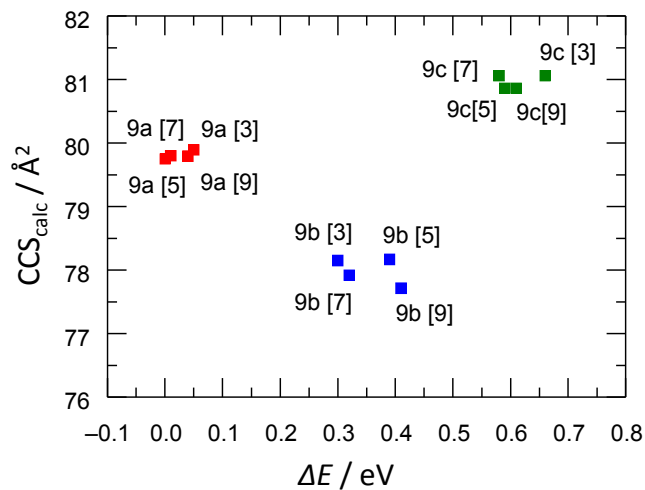


Fig. S2. Dependence of CCS_{calc} of Ir_9^- on isomers and spin multiplicities. Filled red, blue, and green squares are CCS_{calc} of **9a**, **9b**, and **9c**, respectively. The numbers in brackets represent spin multiplicities.

Table S2. Relative energies, AEAs, and VDEs of iridium cluster anions, Ir_n^- ($n = 6$ –8, and 10) with different spin multiplicities obtained with Gaussian09. Certain spin multiplicities and corresponding AEA_{cal} and VDE_{cal} with the lowest relative energy are shown as bolds.

Isomers (even)	spin multiplicity							
	2	4	6	8	10	12	14	16
6a			0.59	0.00	0.20	0.09	0.15	–
AEA_{cal}	–	–	2.12	2.71	2.48	2.59	2.70	–
VDE_{cal}	–	–	2.55	2.88	2.67	2.82	2.83	–
8a	0.15	0.04	0.06	0.00	0.10	–	–	–
AEA_{cal}	2.69	2.79	2.71	2.73	2.59	–	–	–
VDE_{cal}	2.71	2.87	2.70	2.73	2.58	–	–	–
10a	0.41	0.24	0.06	0.00	0.27	–	–	–
AEA_{cal}	2.71	2.74	2.84	2.74	2.47	–	–	–
VDE_{cal}	3.07	2.93	2.90	2.79	2.53	–	–	–
Isomers (odd)	spin multiplicity							
	7	9	11	13	15	17		
7a	0.62	0.35	0.14	0.19	0.00	1.02		
AEA_{cal}	2.43	2.35	2.57	2.43	2.50	1.48		
VDE_{cal}	2.56	2.47	2.65	2.71	2.85	1.54		

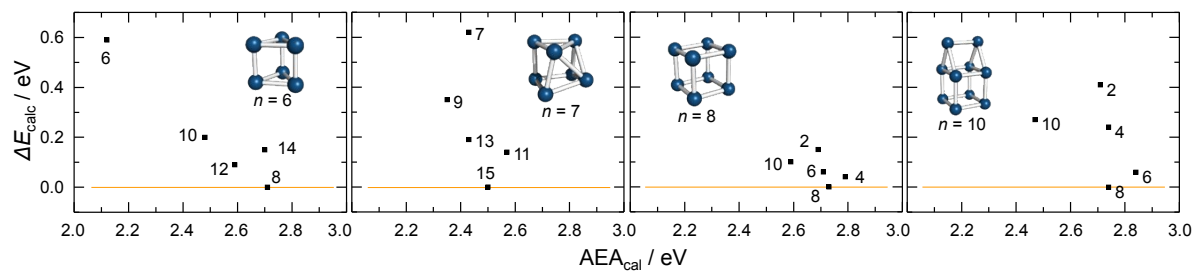


Fig. S3. Plots of relative energies and AEAs of iridium cluster anions, Ir_n^- ($n = 6$ –8, and 10) with different spin multiplicities obtained with gaussian09.

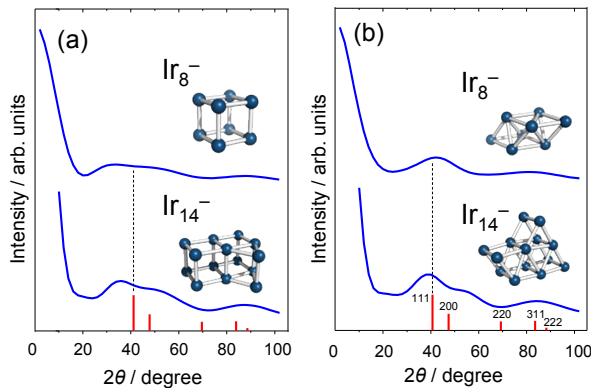


Fig. S4. Simulated XRD pattern of Ir_n ($n = 8$ and 14) with (a) cubic and (b) fcc-like structures.

References

1. Tomihara, R.; Koyasu, K.; Nagata, T.; Wu, J. W. J.; Nakao, M.; Ohshima, K.; Misaizu, F.; Tsukuda, T. *J. Phys. Chem. C* **2019**, *123*, 15301–15306.
2. Ohshima, K.; Komukai, T.; Moriyama, R.; Misaizu, F. *J. Phys. Chem. A* **2014**, *118*, 3899–3905.
3. Tomihara, R.; Koyasu, K.; Tsukuda, T. *J. Phys. Chem. C* **2017**, *121*, 10957.
4. Ho, J.; Ervin, K. M.; Lineberger, W. C. *J. Chem. Phys.* **1990**, *93*, 6987.
5. TURBOMOLE, V7.2; University of Karlsruhe and Forschungszentrum Karlsruhe GmbH (1989–2007) and TURBOMOLE GmbH (since 2007), 2017; available from <http://www.turbomole.com> (accessed Sep. 2019).
6. Waldt, E.; Hehn, A.-S.; Ahlrichs, R.; Kappes, M. M.; Schooss, D. *J. Chem. Phys.* **2015**, *142*, 024319.
7. Frisch, M. J.; Trucks, G. W.; Schlegel, H. B.; Scuseria, G. E.; Robb, M. A.; Cheeseman, J. R.; Scalmani, G.; Barone, V.; Mennucci, B.; Petersson, G. A.; Nakatsuji, H.; Caricato, M.; Li, X.; Hratchian, H. P.; Izmaylov, A. F.; Bloino, J.; Zheng, G.; Sonnenberg, J. L.; Hada, M.; Ehara, M.; Toyota, K.; Fukuda, R.; Hasegawa, J.; Ishida, M.; Nakajima, T.; Honda, Y.; Kitao, O.; Nakai, H.; Vreven, T.; Montgomery, J. A., Jr.; Peralta, J. E.; Ogliaro, F.; Bearpark, M.; Heyd, J. J.; Brothers, E.; Kudin, K. N.; Staroverov, V. N.; Kobayashi, R.; Normand, J.; Raghavachari, K.; Rendell, A.; Burant, J. C.; Iyengar, S. S.; Tomasi, J.; Cossi, M.; Rega, N.; Millam, J. M.; Klene, M.; Knox, J. E.; Cross, J. B.; Bakken, V.; Adamo, C.; Jaramillo, J.; Gomperts, R.; Stratmann, R. E.; Yazyev, O.; Austin, A. J.; Cammi, R.; Pomelli, C.; Ochterski, J. W.; Martin, R. L.; Morokuma, K.; Zakrzewski, V. G.; Voth, G. A.; Salvador, P.; Dannenberg, J. J.; Dapprich, S.; Daniels, A. D.; Farkas, Ö.; Foresman, J. B.; Ortiz, J. V.; Cioslowski, J.; Fox, D. J. *Gaussian 09*, Revision C.01, Gaussian, Inc., Wallingford CT, 2013.
8. Gutsev, G. L.; Jena, P.; Zhai, H.-J.; Wang, L.-S. *J. Chem. Phys.* **2001**, *115*, 7935.
9. Glendening, E. D.; Reed, A. E.; Carpenter, J. E.; Weinhold, F. NBO, version 3.1.
10. The PyMOL Molecular Graphics System, version 1.8; Schrödinger, LLC.
11. Mesleh, M. F.; Hunter, J. M.; Shvartsburg, A. A.; Schatz, G. C.; Jarrold, M. F. *J. Phys. Chem.* **1996**, *100*, 16082–16086.